ORIGINAL ARTICLE

Genes,Brain and Behavior

PACAP-expressing neurons in the lateral habenula diminish negative emotional valence

Marjorie R. Levinstein[1,2,3] | David J. Bergkamp[2,4] | Zoë K. Lewis[5] |
Alex Tsobanoudis[5] | Koichi Hashikawa[4,6,7] | Garret D. Stuber[4,6,7] |
John F. Neumaier[1,2,4,7]

[1]Graduate Program in Neuroscience, University of Washington, Seattle, Washington, USA

[2]Department of Psychiatry and Behavioral Sciences, University of Washington, Seattle, Washington, USA

[3]Biobehavioral Imaging and Molecular Neuropsychopharmacology Unit, National Institute on Drug Abuse Intramural Research Program, Baltimore, Maryland, USA

[4]Department of Pharmacology, University of Washington, Seattle, Washington, USA

[5]Department of Biology, University of Washington, Seattle, Washington, USA

[6]Department of Anesthesiology and Pain Medicine, University of Washington, Seattle, Washington, USA

[7]Center for Neurobiology of Addiction, Pain, and Emotion, University of Washington, Seattle, Washington, USA

Correspondence
John F. Neumaier, Psychiatry and Behavioral Sciences, University of Washington, VA Puget Sound Health Care System 1660 S Columbian Way, Seattle, WA 98108, USA.
Email: neumaier@uw.edu

Abstract

The lateral habenula (LHb) is a small, bilateral, epithalamic nucleus which processes aversive information. While primarily glutamatergic, LHb neurons express genes coding for many neuropeptides, such as *Adcyap1* the gene encoding pituitary adenylate cyclase-activating polypeptide (PACAP), which itself has been associated with anxiety and stress disorders. Using Cre-dependent viral vectors, we targeted and characterized these neurons based on their anatomical projections and found that they projected to both the raphe and rostromedial tegmentum but only weakly to ventral tegmental area. Using RiboTag to capture ribosomal-associated mRNA from these neurons and reanalysis of existing single cell RNA sequencing data, we did not identify a unique molecular phenotype that characterized these PACAP-expressing neurons in LHb. In order to understand the function of these neurons, we conditionally expressed hM$_3$Dq DREADD selectively in LHb PACAP-expressing neurons and chemogenetically excited these neurons during behavioral testing in the open field test, contextual fear conditioning, sucrose preference, novelty suppressed feeding, and conditioned place preference. We found that Gq activation of these neurons produce behaviors opposite to what is expected from the LHb as a whole—they decreased anxiety-like and fear behavior and produced a conditioned place preference. In conclusion, PACAP-expressing neurons in LHb represents a molecularly diverse population of cells that oppose the actions of the remainder of LHb neurons by being rewarding or diminishing the negative consequences of aversive events.

KEYWORDS
Adcyap1, behavior, conditioned place preference, DREADD, fear learning, gene expression, lateral habenula, PACAP, RiboTag, RTqPCR

1 | INTRODUCTION

The lateral habenula (LHb) is a small, bilateral epithalamic nucleus that borders the more diverse medial habenula, projects to a variety of targets, responds to aversive stimuli and promotes avoidances of future adverse events.[1–4] The LHb receives afferents from many forebrain regions, and it is thought to act as a key integrator of information about aversive events that shapes decisions regarding approach or avoidance of similar stimuli in the future.[5,6] These inputs seemed to be biased toward synapsing onto certain efferent pathways. For example, neurons projecting to the LHb from the entopeduncular nucleus preferentially synapse onto neurons projecting to the ventral tegmental area (VTA).[7] LHb outputs directly and indirectly modulate dopaminergic and serotonergic function through its projections to the VTA, raphe, particularly the dorsal raphe nucleus (DRN), and rostromedial tegmental nucleus (RMTg).[8] In general, stimulation of LHb neurons promotes avoidance[1,9] while inhibiting the LHb, or its connections to DRN, VTA or RMTg, reduces anxiety- and depression-like behaviors.[8,10–12] Using virally mediated gene transfer of the inhibitory DREADD receptor, hM$_4$Di, we previously found that inhibiting LHb neurons decreases passive coping in the forced swim test (FST), a measure of behavioral despair, in rats.[13] Furthermore, the LHb neurons projecting to the DRN appear to be responsible for this behavioral effect.[14]

Moreover, the LHb is involved in updating outcome predictions that impact behavioral stability or flexibility.[15] Inactivation of the LHb causes trained rats to perform at a chance level in a tone-directed maze task, indicating the LHb's involvement in adaptive learning and decision making.[16] Lesions of the LHb significantly decreased a win-stay strategy but did not affect lose-shift strategy in a competitive choice task.[17] Additionally, the LHb has been found to be involved in fear learning and memory.[18] Chemogenetic inhibition of rat LHb during conditioning reduced subsequent freezing to contextual cues, but increased freezing in response to discrete cues associated with an aversive stimulus (footshock).[18] Thus, LHb has numerous impacts that can shift the pattern of conditioned responses and decision making in the face of potential aversive outcomes.

Physiological responses of neurons in the LHb are heterogeneous. In the absence of threats, LHb neurons are relatively inactive, firing at roughly 5 Hz,[19] but LHb bursts in response to aversive stimuli such as restraint stress or footshock[20–22] or the absence of an expected reward.[23] Stress exposure also activates LHb neurons intensely and induces c-Fos, a marker of neuronal activity,[24] and chronic unpredictable stress increases firing rates.[19] However, different LHb neurons respond diversely to the same stimulus—about 30% of neurons in the LHb are activated by inescapable footshock,[4] many do not respond at all and roughly 10% of neurons, mostly in the medial region of the LHb, are inhibited by footshock.[20] The basis for these distinctions in responses to stress are not yet understood.

Molecular diversity between LHb neurons has been identified in several ways. First, LHb neurons that project to three primary targets, DRN, VTA, and RMTg are highly segregated with minimal collateral branching.[3,25–29] Using intersectional expression of RiboTag to immunopurify ribosome-associated mRNAs selectively from each of these pathways in rats, we previously identified only small differences in gene expression between the neurons comprising these three pathways, suggesting that the regional target of LHb neurons is not defined by distinctions in neuronal phenotype.[30] LHb neurons are mostly glutamatergic, but numerous neuropeptides are also expressed in these neurons and these may be important in generating different patterns of output activity.[31] Recent gene array and single cell RNA sequencing studies in mice identified several clusters of similar neurons within LHb. While these clusters displayed some topographical bias between cell types, these were not wholly segregated into anatomical regions or pathways targeting distinct brain regions. Nevertheless, these modules of neurons with distinct patterns of gene expression may still have functional implications.[32] For example, a sparsely distributed population of neurons located in the rostromedial region of the LHb expresses the neuropeptide pituitary adenylate cyclase-activating polypeptide (PACAP, encoded by the *Adycap1* gene), which is also expressed in several other brain regions and is particularly abundant in stress-associated nuclei.[33,34] PACAP has been implicated in both stress and addiction[35,36] and regulates cellular signaling, protects from oxidative stress, and has organism-wide effects, such as activating the hypothalamic–pituitary–adrenal hormone system in response to stress[37] although previous studies have focused on other brain areas, such as the extended amygdala. Chronic stress increases PACAP expression in the bed nucleus of the stria terminalis, a brain region associated with anxiety.[38] Moreover, PACAP infusion increases freezing and other anxiety-like behaviors.[39,40] A single nucleotide polymorphism of the cognate receptor for PACAP, *ADCYAP1R1*, is associated with increased likelihood of developing posttraumatic stress disorder in adult women and female children.[41,42] While stress and the neuropeptide PACAP have a well-studied relationship, the role of PACAP-expressing neurons in the LHb on stress-related behaviors has not been investigated.

Therefore, in this study, we examined PACAP-expressing neurons in LHb in greater detail using a combination of transgenic PACAP-promoter Cre mice injected with a viral vector carrying a floxed hM$_3$Dq DREADD receptor, allowing precise chemogenetic activation of PACAP neurons in LHb. We found that these neurons do not represent a distinct cluster of molecularly unique cells but chemogenetic activation of these neurons produced a paradoxical pattern of conditioned place preference and reduced fear and anxiety-associated behaviors.

2 | METHODS

2.1 | Animals

Adcyap1-2a-Cre recombinase (PACAP-Cre) transgenic mice (C57BL/6 background)[43] were bred to C57BL/6 wildtype mice creating PACAP-Cre and wildtype littermates. Litters were genotyped, and only transgenic mice were used except for six wildtype littermates that were used as negative controls for RiboTag expression; males and females

were housed in separate cages. One hundred and eleven PACAP-Cre mice were placed in groups that were age matched with littermate controls. Mice ranged in size from 25 to 30 gm and were between 3 and 6 months old at the time of experiments. Mice were group housed in a temperature- and humidity-controlled vivarium with a 14–10 light–dark cycle and fed ad libitum. Experiments were performed during the light phase in compliance with the Guide for the Care and Use of Laboratory Animals (NIH, 1985; Publication 865–23) and were approved by the Institutional Animal Care and Use Committee, University of Washington. Live decapitation was used for RiboTag RNA Isolation procedures, while paraformaldehyde (PFA) perfusion was conducted for immunohistochemistry.

2.2 | Surgical procedures

For stereotaxic surgeries, anesthesia was induced with 3% isoflurane/97% oxygen and maintained at 1% isoflurane during the surgical procedure. Using a custom robotic stereotaxic instrument,[44] mice were injected with AAV8-DIO-hM$_3$Dq-2a-RiboTag ($n = 32$), AAV8-DIO-hM$_3$Dq-mcherry ($n = 10$), a 50/50 combination of AAV8-DIO-hM$_3$Dq-mcherry and AAV8-hSyn-DIO-RiboTag ($n = 13$), AAV8-hSyn-DIO-RiboTag alone ($n = 44$), or AAV1-DIO-Synaptophysin-GFP ($n = 3$) into LHb. Blunt 28 g needles were inserted bilaterally, terminating at A/P -1.85, M/L ±0.35, and D/V −2.59, and 0.5 μL of the virus was injected at a rate of 0.2 μL/min. Five additional mice were injected unilaterally with AAV1-DIO-Synaptophysin-EGFP using a beveled NanoFil needle (33 g, WPI) terminating at A/P −1.85 mm, M/L +0.33 mm, and D/V −2.59 mm. The needle opening faced medially toward the center of the LHb. The needle was left in situ for 5 minutes post-injection then slowly withdrawn. After surgeries, mice were given meloxicam (0.5 mg/kg, s.c.) for analgesia and monitored daily for at least 3 days. Accuracy of injection coordinates was confirmed by RTqPCR detection of RiboTag and Cre RNAs from LHb homogenate; these injection volumes and coordinates were optimized to produce selective transduction of LHb neurons with minimal expression adjacent regions.

2.3 | Plasmid and reagents

The hSyn-hM$_3$Dq-2A-RiboTag construct was generated using Gibson Assembly (NEB, Ipswich, MA) following PCR amplification of hM$_3$Dq sequence from pAAV-hSyn-DIO-hM$_3$D(Gq)-mCherry (Plasmid #44361, Addgene, Cambridge, MA); sequence fidelity was confirmed by sequencing. The 2A-skip sequence (ATNFSLLKQAGDVEENPGP) and RiboTag construct were PCR amplified from pcDNA3-hSyn-mRuby2-2A-RiboTag.[45] The flag sequence was (DYKDDDDK) was introduced using overlapping oligonucleotides. The final viral construct was sent to the Fred Hutchinson Cancer Research Center Co-Operative Center for Excellence in Hematology Vector Production Core and was packaged in an adeno-associated virus 8 (AAV8) capsid. Clozapine-N-Oxide (CNO) was provided by the NIDA Drug.

2.4 | Anterograde tracing

PACAP-Cre mice injected with AAV1-DIO-Synaptophysin-GFP were allowed to rest for 3 weeks for expression to develop. Mice were deeply anesthetized with Beuthanasia-D (diluted by 50% in saline, 4 mL/kg ip, Merck Sharp & Dohme Corp) and perfused with ice cold physiological saline, followed by 4% PFA in PBS. Brains were then extracted and stored in 4% PFA in PBS overnight, followed by cryoprotection in 30% sucrose. Brains were then sliced at 40 μm in preparation for immunohistochemistry. Slices were incubated in 4% BSA and 0.03% triton in PBS blocking solution for 1 h at room temperature. PBS rinses were performed between each step 6 times for 10 min each. Following blocking incubation, slices were incubated in primary antibodies diluted at 1:2000 for chicken anti-GFP (Abcam, ab13970), 1:1000 for goat anti-TPH2 (Millipore Sigma, #ABN60), and 1:500 for rabbit anti-GAD65/67 (Abcam, ab183999) in blocking buffer at 4°C, shaking for 72 h. For negative controls, primary antibodies were omitted from the incubation. Slices were washed following the primary antibody incubation step and then incubated with 1:1000 Alexa Fluor 488 anti-chicken (Thermo Fisher, A-11039), 1:1000 Alexa Fluor 568 anti-rabbit (Thermo Fisher, A-11036), and 1:1000 Alexa Fluor 647 anti-goat (Thermo Fisher, A-21447) at room temperature, shaking for 2 h. Slices were then washed again, mounted onto slides, and treated with DAPI to stain cell nuclei (Thermo Fisher, P36966) in ProLong Diamond mounting medium. Slides were allowed to cure for 24 h in the dark at room temperature before imaging.

2.5 | Imaging

For the bilaterally injected mice, dual-channel (GFP, excitation 450–490, emission 500–550; DAPI, excitation 335–383, and emission 420–470) images were collected on a high-content fluorescent microscopy system (Zeiss Axio Imager M2, constant exposure settings for all experiments) using a 20× objective. All images were collected using Axiocam MRC camera.

For the five unilaterally injected mice, all sections were first imaged at 4× and 40× using a computer controlled, widefield microscope (Keyence BZ-X2000). For some slices of interest, further imaging was performed at 40× (dry) and 63× (oil immersion) using a confocal scanning microscope (Leica TCS SP8). For z-stack images, imaging of the four separate channels was carried out in two separate series using a HyD detector and a PMT detector (2 channels per series scan) using 3× frame and 3× line averaging. The pinhole was set to an Airy unit of 1 at 568 nm and the best scan thickness was determined by the Leica XPS software for 10–20 μ thick planes. All confocal images were taken at 1024 × 1024 pixel resolution or greater while performing bidirectional scanning.

2.6 | Ribotag extraction

RiboTag-associated RNA extraction as previously described.[30,46,47] The LHb was extracted using a midline 3 mm punch and homogenized in 1 mL of supplemented homogenizing buffer [S-HB, 50 mM Tris–HCl, 100 mM KCl, 12 mM MgCl2, 1% NP40, 1 mM DTT, $1\times$ Protease inhibitor cocktail (Sigma-Aldrich), 200 U/mL RNasin (Promega, Madison, WI), 100 μg/mL cyclohexamide (Sigma-Aldrich), 1 mg/mL heparin (APP Pharmaceuticals, Lake Zurich, IL)]. Samples were centrifuged at $4°C$ at $11,934 \times g$ for 10 min, and supernatant was collected, reserving 50 μL (10%) as an input fraction. Mouse monoclonal HA-specific antibody (2.5 μL) (HA.11, ascites fluid; Covance, Princeton, NJ) was added to the remaining supernatant, and RiboTag-IP fractions were rotated at $4°C$ for 4 h. Protein A/G magnetic beads (200 μL) (Pierce) were washed with Homogenizing Buffer (HB, 50 mM Tris–HCl, 100 mM KCl, 12 mM MgCl2, 1% NP40) prior to addition to the RiboTag-IP fraction and were rotated at $4°C$ overnight. The next day, RiboTag-IP fractions were placed on a DynaMag-2 magnet (Life Technologies), and the bead pellet was washed three times for 15 min with high salt buffer (HSB; 50 mM Tris, 300 mM KCl, 12 mM MgCl2, 1% NP40, 1 mM DTT, and 100 μg/mL cyclohexamide) and placed on a rotator. After the final wash, HSB was removed and beads were re-suspended in 400 μL supplemented RLT buffer (10 μL β-mercaptoethanol/10 mL RLT Buffer) from the RNeasy Plus Micro Kit (Qiagen, Hilden, Germany) and vortexed vigorously. These samples were then placed back on the magnet and the RLT buffer was removed from the magnetic beads prior to RNA extraction. 350 μL supplemented RLT buffer was added to the Input Fraction prior to RNA extraction. RNA from the Input Fraction was extracted using Qiagen RNeasy Plus Mini kit (Qiagen, Hilden, Germany) and RNA from the RiboTag-IP fration was extracted using Qiagen RNeasy Plus Micro kit according to package directions. Input RNA was eluted with 40 μL of water and RiboTag-IP RNA was eluted with 14–16 μL of water. RNA concentration was measured using Quant-iT RiboGreen RNA Assay (ThermoFisher Cat. R11490, Waltham, MA).

2.7 | RT-qPCR analysis

The RNA was reverse transcribed to create cDNA libraries for qPCR using Superscript VILO Master Mix (ThermoFisher Cat. 11754050, Waltham, MA), and then cDNA libraries were diluted to a standard concentration before running the qPCR assay using Power Sybr Green on a QuantStudio 7 Real-Time PCR System (Thermo Fisher). Standard curves were created by pooling RNA from input sample following a two-fold serial dilution. Relative starting transcript quantity (RSTQ) was calculated based on Ct-values of Standard Curve Samples for each series of experiments. For all analyses except for direct measurement of housekeeping genes (*Hprt*, *Ppia*, *Gapdh*, and ß-*Actin*), expression was normalized using these housekeeping genes. Normalization factors were generated based on average housekeeping levels for RiboTag-IP fractions and Input fractions independently. Normalized RSTQ data was analyzed using ANOVA with the Bonferroni post-hoc

test. Enrichment was determined by dividing Normalized RSTQ of IP by the corresponding Normalized RSTQ input value. Neuronal activation and pulldown were determined using primers specific for *c-fos*, RiboTag, and Cre recombinase. Genes of interest were determined from clusters determined by integrative expression matrices of single cell RNAseq (scRNAseq) data.[32] *Adcyap1* was most commonly expressed in LHb5 and LHb1 clusters. Clusters and *Adcyap1* expression were visualized using Uniform Manifold Approximation Projection (UMAP). The genes from these clusters with the most (*Lbhd2*, *Dlgap1*, and *Rgs4*) and least (*Id4*, *Sncg*, and *Nek7*) overlap of cells expressing Adcyap1 were tested. Primer sequences can be found in Supplementary Table S1.

2.8 | Behavioral experiments

2.8.1 | Open field

PACAP-Cre Mice that received an injection of AAV8-DIO-hM₃Dq-mCherry were given an injection of CNO 3 mg/kg ip ($n = 5$) or vehicle ($n = 5$) 30 minutes prior to placement in the open field chamber (50 cm × 50 cm). The mice were allowed to freely explore the chamber while being video recorded for 20 min. Ninety minutes after the CNO or vehicle injection, mice were perfused and tissue treated as described below. Videos were scored using Ethovision.

2.8.2 | Sucrose preference

PACAP-Cre mice that received an injection of AAV8-DIO-hM₃Dq-2a-RiboTag ($n = 20$) or AAV8-DIO-RiboTag ($n = 18$) were placed in 2-bottle choice lickometer chambers for 3 h and given free access to a bottle of water and a bottle of 2% sucrose solution to allow for habituation. The next day, mice received an injection of CNO 3 mg/kg ip or vehicle 30 min prior to being placed back inside the two bottle choice lickometer chambers for 3 h and given free access to a bottle of water and a bottle of 2% sucrose solution. Sucrose and water bottle sides were counterbalanced between animals, and licks were automatically counted.

2.8.3 | Novelty suppressed feeding

This procedure was performed as described[48,49] in PACAP-Cre mice injected with either AAV8-DIO-hM₃Dq-2a-RiboTag ($n = 20$) or AAV8-DIO-RiboTag ($n = 18$). The testing chamber was a plastic box (50 × 50 × 20 cm), the floor of which was covered with approximately 2 cm of corncob bedding, with illumination of 1200 lux. Eighteen hours before behavioral testing, all food was removed from the home cage. 30 min prior to behavioral testing, mice received an injection of CNO 3 mg/kg or vehicle *ip*. At the time of testing, a single pellet of food was placed on a white paper platform in the center of the box and secured with a rubber band. The mouse was placed in a

corner of the box and a stopwatch was immediately started. The latency to eat (defined as the mouse sitting on its haunches and biting the pellet with the use of forepaws) was timed. Mice were in the testing arena for a total of 8 min. Immediately after the testing period, the mice were transferred to their home cages, and the amount of food consumed by the mouse in the next 5 min was measured. Each mouse was weighed before food deprivation and before testing to assess the percentage of body weight loss.

2.8.4 | Contextual fear conditioning

Behavior was performed three to 4 weeks after viral vector infusion (either AAV8-DIO-hM$_3$Dq-2a-RiboTag ($n = 32$), or AAV8-DIO-hM$_3$Dq-mcherry + AAV8-DIO-RiboTag ($n = 13$), or AAV8-DIO-RiboTag ($n = 44$)). Acquisition of fear memory was conducted in four identical chambers (21.6 × 17.8 × 12.7 cm; Med Associates) placed inside sound-attenuating boxes. Each chamber was made of two aluminum and two Plexiglas side walls. The floor consisted of 24 stainless steel rods which were wired to a scrambled shock generator. To add a context-specific odor, the chamber was cleaned with a 1% acetic acid solution between mice and a stainless-steel pan containing the same solution was placed under the grid floor.[50] For fear training, mice received an injection of CNO 3 mg/kg or vehicle *ip* 30 min prior to being placed in the middle of the test cage and allowed to acclimate for 2 min, then received three 1 s, 0.6 mA footshocks at two-minute intervals. Following the third and final footshock, mice remained in the test cage for an additional minute before being returned to their home cage. After 24 h, mice were placed back in the test cage for a five-minute test session. Training and testing sessions were digitally recorded, and freezing was analyzed by reviewing the recorded sessions offline.

2.8.5 | Conditioned place preference

PACAP-Cre mice, with either AAV8-DIO-hM$_3$Dq-2a-RiboTag ($n = 11$) or AAV8-DIO-hM$_3$Dq-mcherry + AAV8-DIO-RiboTag ($n = 13$) for experimental mice and AAV8-DIO-RiboTag ($n = 25$) for control mice were tested for preference or aversion to CNO in a two-chamber apparatus with distinct visual and tactile cues as described previously.[51] All conditioning and testing sessions lasted 30 min and were recorded on video for analysis in Ethovision version 3.0 (Noldus). On day 1 (pretest), mice freely explored each side of the apparatus. Total time on each side was calculated and mice were then conditioned with CNO (3 mg/kg *ip*) paired on either the preferred or not preferred side in a balanced (unbiased) manner. On days 2 and 3 (conditioning), mice were confined to one side with saline treatment and, >4 h later, confined to the other side starting 5 min after CNO administration. On day 4, mice were allowed to freely explore each side of the apparatus and time spent on the drug-paired floor during the test was measured. Preference score was determined by subtracting time on the drug-paired

compartment during posttest from time on the drug-paired compartment during pretest (post–pre).

2.9 | Statistical analysis

All data were analyzed using Graphpad Prism 9 using 2-way ANOVA or independent t-tests where appropriate.

2.10 | Data availability

The data that support the findings of this study are available from the corresponding author upon reasonable request.

3 | RESULTS

3.1 | Fiber tracing

There are three dominant output pathways from LHB: to the DRN, VTA, and RMTg. Therefore, we injected three male PACAP-Cre mice with AAV1-DIO-Synaptophysin-GFP bilaterally into the LHb to evaluate the projection pattern for these neurons (Figure 1A). Anterograde tracing of PACAP neurons showed strong Synaptophysin-EGFP expression in the DRN, and RMTg, but weaker to the VTA. Specifically, the lateral wings of the DRN showed innervation by bulbous puncta and fibers to a greater extent than the center of the DRN. The RMTg showed strong innervation by PACAP neurons, as did the ventral portion of the Pons.

Staining for GFP, Tph2, and GAD65/67 showed that a few cells in the DRN displayed expression of both Tph2 and GAD, but most cells were positive for one or the other. The expression pattern of GFP suggested that beaded fibers of PACAP releasing axons were present in the DRN in the lateral wings, the center of the DRN, and in the ventral portion of the pons. GAD65/67 staining was most intense in the wings of the DRN, but also showed significant expression in the periaqueductal gray and the pons, as well as the cortex and cerebellum. The GFP expressing axons showed clear proximity to both Tph2 expressing neuronal cell bodies as well as GAD65/67 expressing cell bodies and puncta, which suggests that PACAP expressing cell axons could potentially release the peptide onto GAD65/67 expressing interneurons within the DRN.

3.2 | Molecular characterization of PACAP neurons

Since PACAP-expressing neurons did not segregate into a single projection pathway, we next considered whether these neurons mapped onto a clustering scheme derived from scRNAseq from our recent report.[32] The expression level of *Adcyap1* was visualized in UMAP space. As shown in Figure 2A, the clusters with the largest percentage
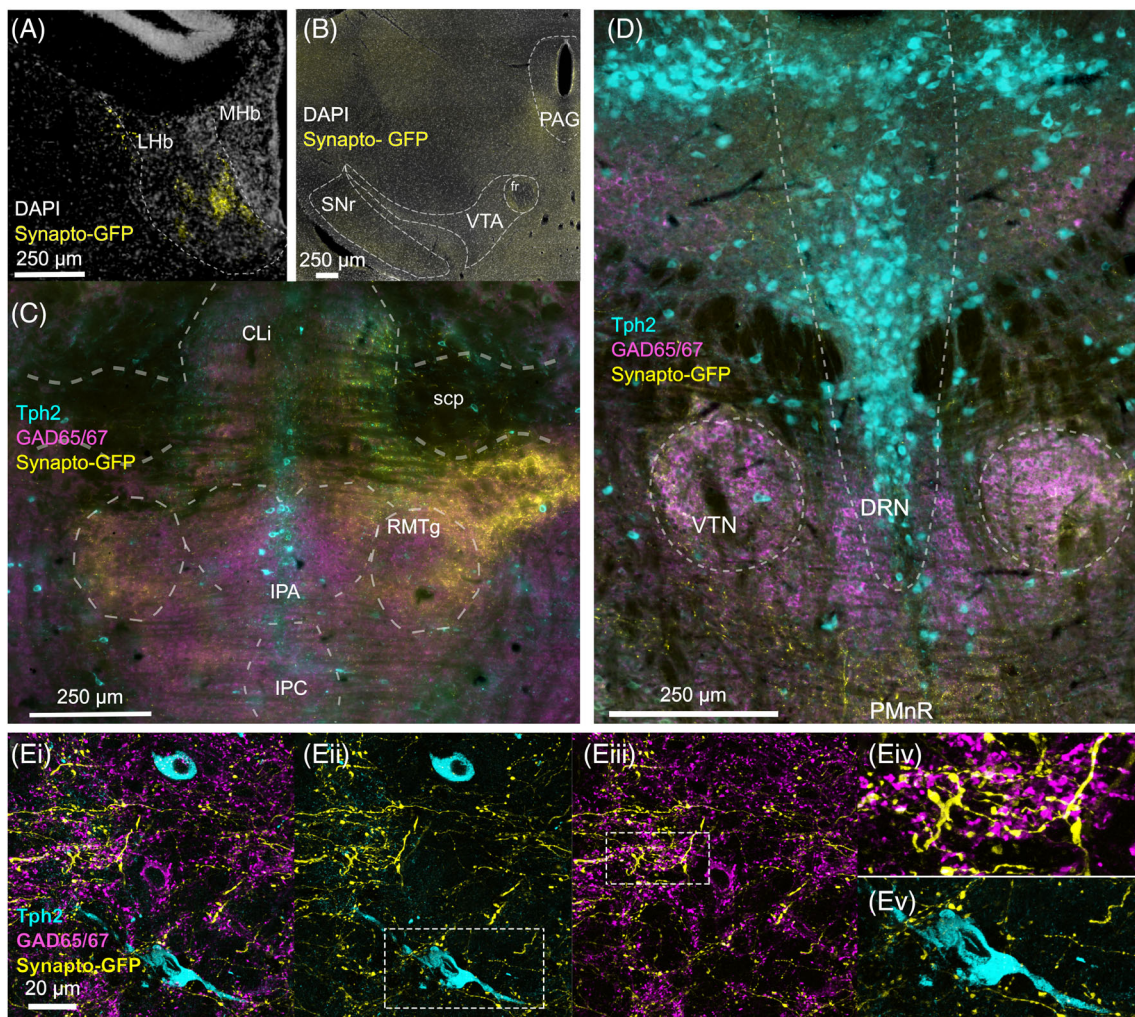
FIGURE 1 PACAP neurons in the LHb project to DRN and RMTg, but not VTA. AAV1-DIO-Synaptophysin-GFP was injected into LHb of PACAP-Cre mice to express GFP in terminals of infected neurons, shown here in yellow. Synapto-GFP expression at the site of viral injection in LHb (A). The VTA and SNr of the same mouse shown in B did not contain Synapto-GFP expressing fibers (B). An anterior section stained for tryptophan hydroxylase 2 (Tph2, cyan) and GAD65/67 (magenta) contains Synapto-GFP expressing LHb efferents in the RMTg and an anterior portion of the interpeduncular nucleus (IPA) (C). Similar staining in a more posterior section show innervation of the DRN and upper portion of the paramedial raphe (PMnR); efferent fibers expressing Synapto-GFP are adjacent to both serotonergic and GABAergic neurons (D). Maximum projection of confocal z-stack image (3.5 μ thick) of a portion of the lateral wings of the DRN (separate section from those shown above) (E_i) details the extent to which GFP labeled fibers from the LHb (E_{ii}) lie in close proximity to cells expressing either GAD65/67 (E_{iii-iv}) and Tph2 (E_v)

of PACAP-positive neurons were LHb5 and LHb1, although there were some PACAP-positive neurons in the other clusters as well. We next injected AAV8-DIO-RiboTag virus into LHb of PACAP-cre mice so that we could retrieve ribosome-associated RNAs that were actively being translated by PACAP-expressing neurons. Using RTqPCR, we examined several RNA targets chosen for their relative enrichment or de-enrichment in LHb1 and LHb5 neuron clusters as compared to the other clusters. We determined enrichment by dividing Normalized RSTQ of IP by the corresponding Normalized RSTQ input value. As shown in Figure 2B–I, neither the type of virus, nor the administration of CNO the previous day affected the enrichment values of any of these RNAs (*Lbhd2* (interaction: $p = 0.881$, virus construct: $p = 0.295$, drug treatment: $p = 0.690$), *Dlgap1* (interaction: $p = 0.789$, virus construct: $p = 0.492$, drug treatment: $p = 0.058$),

Rgs4 (interaction: $p = 0.942$, virus construct: $p = 0.135$, drug treatment: $p = 0.224$), *Id4* (interaction: $p = 0.094$, virus construct: $p = 0.628$, drug treatment: $p = 0.865$), *Sncg* (interaction: $p = 0.269$, virus construct: $p = 0.261$, drug treatment: $p = 0.993$), and *Nek7* (interaction: $F_{1,17} = 4.75$, $p = 0.044$, virus construct: $p = 0.355$, drug treatment: $p = 0.972$). Based on the scRNAseq data, we expected *Lbhd2*, *Dlgap1*, and *Rgs4* to be enriched and *Id4*, *Sncg*, and *Nek7* to be de-enriched in PACAP neurons as compared to input RNA after collapsing across treatment groups,, but none of these RNAs were enriched in RiboTag purified RNA from PACAP-Cre neurons as compared to the input RNA from the tissue punches although several were de-enriched (*Lbhd2* (enrichment mean $= 0.540$, $t(20) = 7.001$, $p < 0.001$), *Dlgap1* (enrichment mean $= 0.405$; $t(20) = 8.694$, $p < 0.001$), *Rgs4* (enrichment mean $= 0.509$; $t(20) = 7.767$, $p < 0.001$),
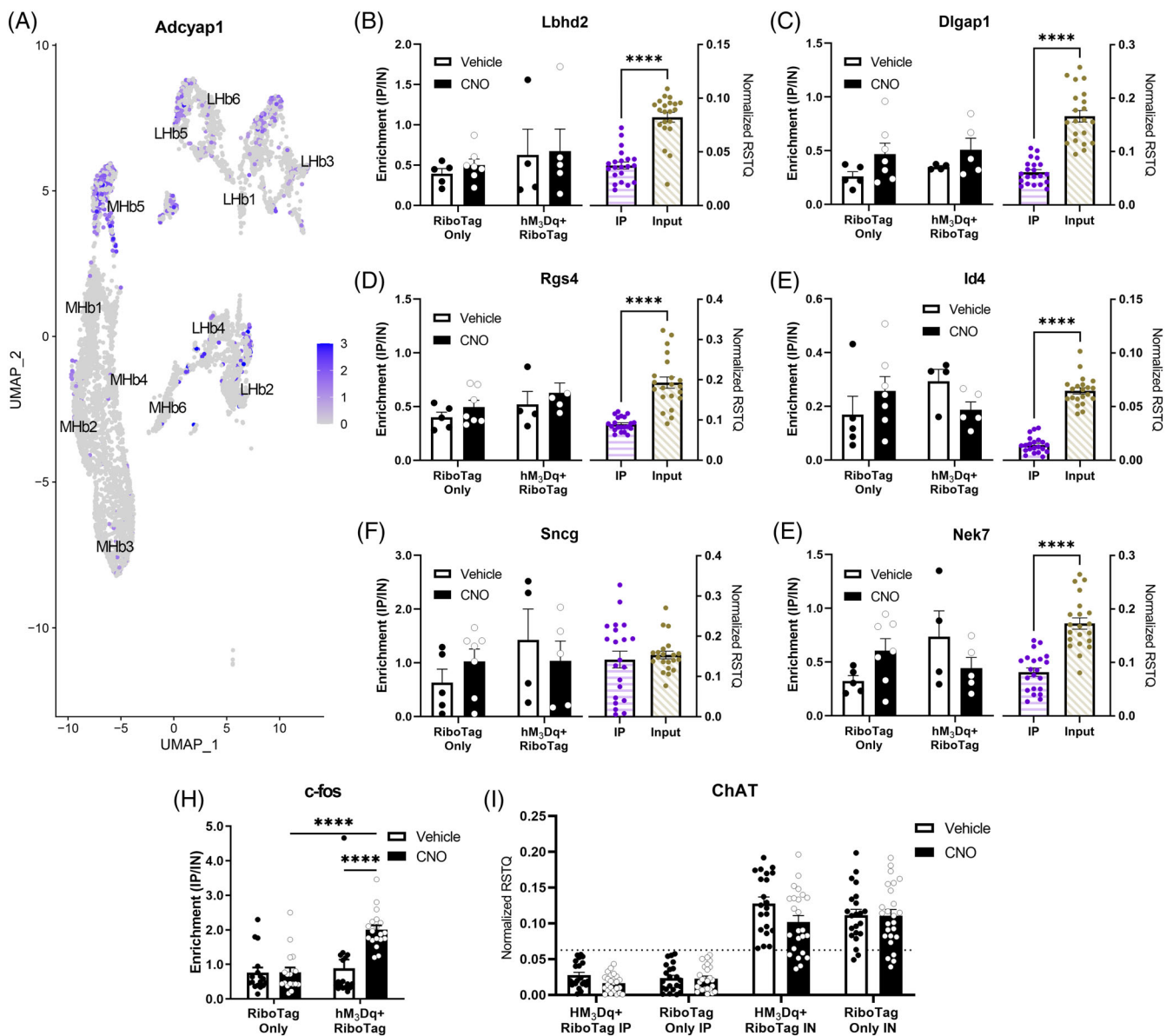
FIGURE 2 PACAP is expressed across multiple phenotypically clustered LHb neurons. (A) UMAP plot of PACAP expressing neurons (displayed in purple) shows that PACAP expression is distributed across the six clusters of LHb neurons defined by scRNAseq. Scale bar represents relative expression. By expressing RiboTag in LHb PACAP-Cre neurons, we examined several genes that were strongly associated with neurons that expressed PACAP in the scRNAseq dataset--Lbhd2(B), Dlgap1(C), and Rgs4 (D), and genes that were predicted to be de-enriched in PACAP neurons—Id4 (E), Sncg (F), and Nek7 (G). In all of these cases we examined both PACAP-RiboTag-only mice and PACAP-hM$_3$Dq mice after treatment with vehicle or CNO (3 mg/kg ip) the previous day and observed no significant effect of DREADD activation on expression of these genes or effect of CNO in mice lacking hM$_3$Dq (left graph of each panel). Most of these genes were de-enriched (right graph of each panel). CNO 50 min prior to sacrifice increased *c-fos* expression dramatically in PACAP-hM$_3$Dq mice but not PACAP-RiboTag only mice (H), indicating that both the Gq DREADD receptor and the RiboTag protein were functionally expressed in these neurons. ChAT expression was below the limit of our standard curve (dotted line) in the IP samples, but not their corresponding inputs (I)

Sncg (enrichment mean = 1.010; t (20) = 8.694, p = 0.642), and *Nek7* (enrichment mean = 0.524; t (20) = 6.672, p < 0.001)); however, *Id4* (enrichment mean = 0.226; t (20) = 15.48, p < 0.001) (Figure 2E) was particularly de-enriched relative to the input RNA, suggesting that it is less abundant in PACAP neurons in LHb. Thus, we conclude that PACAP-expressing neurons do not map tightly onto a specific phenotypic cluster of LHb neurons as defined by scRNASeq. Furthermore, stimulation of hM$_3$Dq with CNO the previous day did not alter the

overall pattern of expression of these RNAs (Figure 2). Since the MHb5 cluster also contains PACAP-expressing neurons, we tested whether choline acetyltransferase (ChAT) was detectable in the mice which we injected with RiboTag virus; ChAT RNA in the RiboTag IP samples was very low and below the lowest concentration on our standard curve (Figure 2I); this indicated that our injection procedures were well targeted and specific for LHb over MHb. Together, these results suggest that PACAP-expressing neurons in LHb are widely distributed

and not restricted to a narrow cluster of neurons with a discrete phenotype, although they mostly do not project to VTA.

3.3 | Chemogenetic activation of LHb PACAP neurons

We tested the effects of activating hM_3Dq, the Gq-coupled DREADD receptor,[52,53] when selectively expressed in LHb PACAP neurons. PACAP hM_3Dq mice were sacrificed 50 minutes after an injection of CNO, had significantly more *c-fos* mRNA expression and enrichment than other groups (Figure 2H, Interaction: $F_{1,67} = 10.77$, $p = 0.0016$; hM_3Dq CNO vs hM_3Dq Vehicle (t(67) = 4.697, $p < 0.0001$; vs RiboTag only CNO t(67) = 5.242, $p < 0.0001$). In this and the behavioral chemogenetic experiments, sex differences were investigated by two-way ANOVA; none were found therefore males and females were combined and analyzed together.

3.4 | Behavioral testing after chemogenetic activation of LHb PACAP neurons

3.4.1 | Open field

In a preliminary study, mice which had hM_3Dq expressed in their LHb PACAP neurons (PACAP-hM_3Dq mice) had significantly more locomotion after treatment with CNO than those treated with vehicle (t (8) =4.264, $p = 0.0027$; Figure 3A–C); they also spent significantly less time in the corners (t (8)=2.433, $p = 0.0410$) after CNO (3 mg/kg *ip*) as compared to vehicle (Figure 3D). There were no significant differences in locomotion, center or corner time between males and females.

3.5 | Contextual fear conditioning

In the contextual fear conditioning test, when comparing males and females, there were no sex differences; therefore, the sexes were combined, and groups were analyzed together. On test day, there was a significant Treatment x Virus interaction ($F_{1,78} = 13.25$, $p = 0.0005$) (Figure 3E). PACAP-hM_3Dq mice treated with CNO (3 mg/kg *ip*) froze significantly less than those treated with vehicle (t[78] = 4.366, $p = 0.0002$) or mice injected with AAV8-DIO-RiboTag (PACAP-RiboTag only mice) given CNO (t[78] = 3.234, $p = 0.0107$). Moreover, there were no differences in freezing time between groups on Conditioning Day (Figure 3F).

3.6 | Conditioned place preference

PACAP-hM3Dq mice had a stronger preference for the CNO paired side than PACAP-RiboTag only mice t (42)=3.8951, $p = 0.0003$ (Figure 4A), although there was a trend for a Sex × Virus interaction

($F_{1,40} = 3.81$, $p = 0.0580$) and a trend for a main effect of sex ($F_{1,40} = 3.043$, $p = 0.0888$) when the preliminary 2-way ANOVA was performed which indicated a larger effect in males than females.

3.7 | Sucrose preference and novelty suppressed feeding

There were no differences between males and females in either of these behaviors, so sexes were combined and analyzed together. PACAP hM_3Dq or PACAP RiboTag only mice displayed no differences in sucrose preference with or without CNO (Main effect of virus: $F_{1,36} = 2.843$, $p = 0.1004$; Main effect of treatment: $F_{1,36} = 2.619$, $p = 0.114$; Interaction: $F_{1,36} = 1.705$, $p = 0.200$) (Figure 4B). Nor did they display any differences in latency to bite the pellet (Figure 4C) (Main effect of virus: $F_{1,36} = 0.08071$, $p = 0.778$; Main effect of treatment: $F_{1,36} = 0.07616$, $p = 0.784$; Interaction: $F_{1,36} = 0.1200$, $p = 0.731$) or homecage feeding (not shown) in the novelty suppressed feeding test.

4 | DISCUSSION

In this report we used viral vectors to express DREADD receptor and RiboTag conditionally in PACAP-Cre expressing neurons in LHb to investigate their role in the control of emotional behaviors. In these experiments we found that chemogenetic activation of LHb PACAP neurons increased locomotion, reduced anxiety-like behavior, reduced fear-learning, and may be modestly rewarding. Surprisingly, these results oppose published or predicted results for LHb neuronal function in general. However, activating these neurons did not affect neophobia in the novelty suppressed feeding test, nor did it affect hedonic valence as tested in the sucrose preference test. These results indicate these neurons may be behaving paradoxically compared to the LHb as a whole.

Recently, the LHb was found to be involved in fear memory.[18] Indeed, Durieux and colleagues (2020) found that neurons in the rostral and medial LHb had increased c-Fos expression after fear conditioning compared to rats which remained in their homecage (rats exposed to tone and chambers also had increased c-Fos expression). Chemogenetic inhibition of the LHb prior to conditioning altered conditioned fear later by reducing freezing to contextual cues but increasing freezing when the conditioned stimulus tone was presented in a new context. We found that activating LHb PACAP neurons during conditioning also decreased freezing when contextual cues were presented during the test session, which is consistent with these neurons playing a distinct role compared to LHb neurons in general. It is important to note that these data do not directly implicate PACAP release per se as these neurons also express other transmitters, such as glutamate.

FIGURE 3 Chemogenetic activation of PACAP-expressing neurons in the LHb reduces anxiety and fear behaviors. Representative heatmaps of individual mouse position within the open field from PACAP-hM3Dq mice treated with vehicle (A) or CNO (3 mg/kg *ip*) (B); the heatmap colors indicate time spent at a particular position ranging from blue (least) to red (most). Mice that were injected with CNO traveled a significantly greater distance (C) and spent less time in the corners (D). PACAP-hM3Dq mice and PACAP-RiboTag-only mice treated with vehicle or CNO show similar levels of freezing during the conditioning session in contextual fear conditioning (E), but PACAP-hM3Dq mice given CNO showed reduced freezing when tested the next day compared to vehicle or PACAP-RiboTag only mice (F)
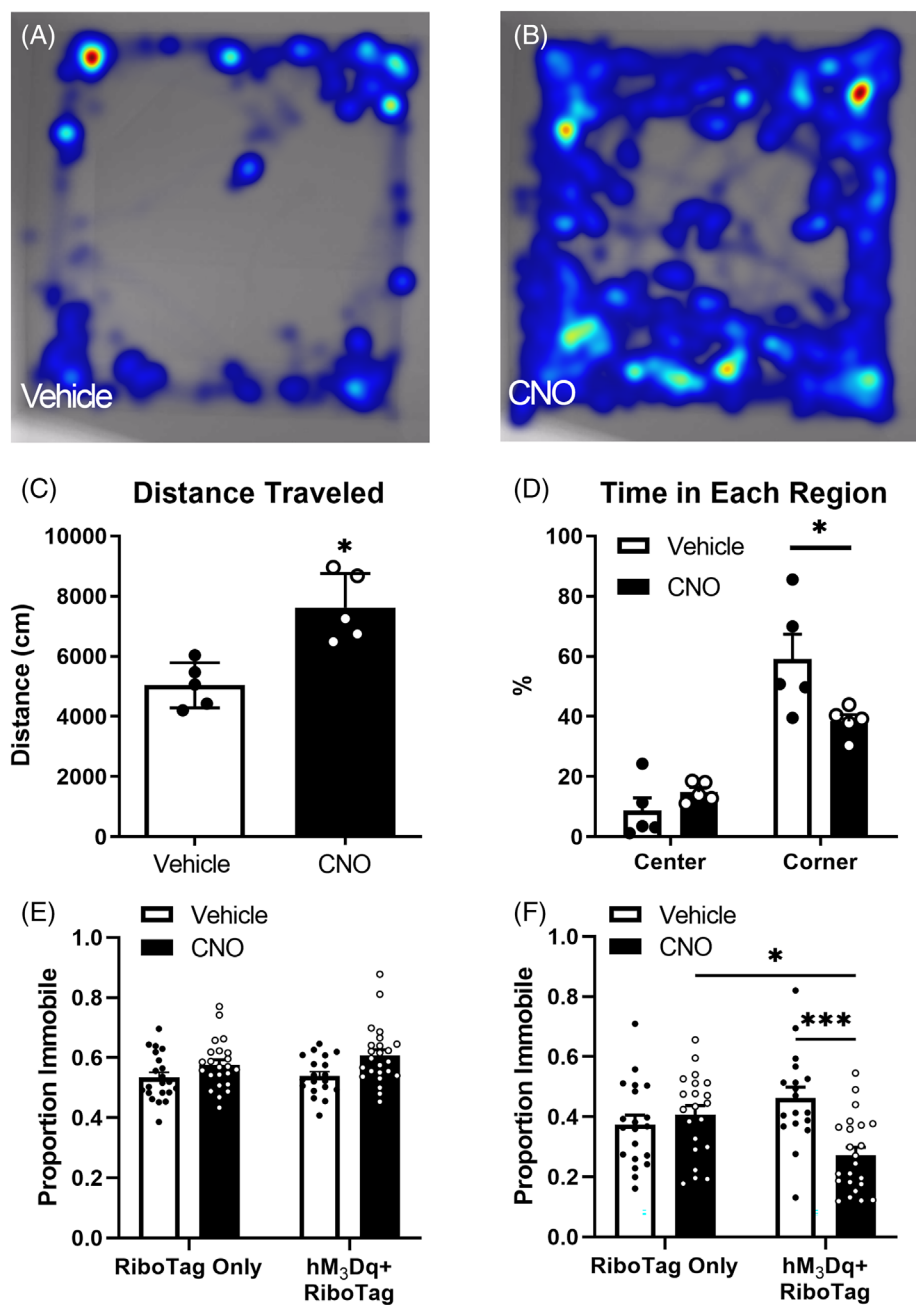
In addition, we investigated the anatomical projections and genetic profile of PACAP-expressing neurons in LHb. We found that these neurons strongly project to the raphe and RMTg, but weakly to the VTA. Thus, these neurons are not specific to one pathway. Interestingly, our data indicate that PACAP-expressing LHb neurons tend to project mainly toward the lateral part of the dorsal raphe and the medial raphe nuclei where GABAergic interneurons reside. However, PACAP-expressing neuronal synapses are adjacent to both serotonergic and GABAergic neurons in this region. Synaptophysin-GFP terminals can be seen in the Pons, medial raphe nucleus, and central DRN as well.

We also leveraged recently published scRNAseq data from the habenula and identified a number of clusters of LHb neurons based on their overall patterns of gene expression.[32] With further analysis of these data, we reveal here that PACAP-expressing neurons were distributed across several previously identified LHb neuronal cell types, especially LHb5 and LHb1, suggesting that PACAP expression itself did not uniquely identify a specific subtype of LHb neurons. In the earlier study, the LHb5 cluster, which had the highest abundance of PACAP-expressing neurons, did not have an induction of immediate early genes by repeated footshocks, indicating that aversive stimuli may not activate this cluster of neurons. In the present study, using the reverse approach of examining RNA expression by PACAP-expressing neurons, we did not identify a unique molecular signature. Thus, PACAP expression does not seem to define these neurons as a unique molecular or anatomical set even though they do seem to have
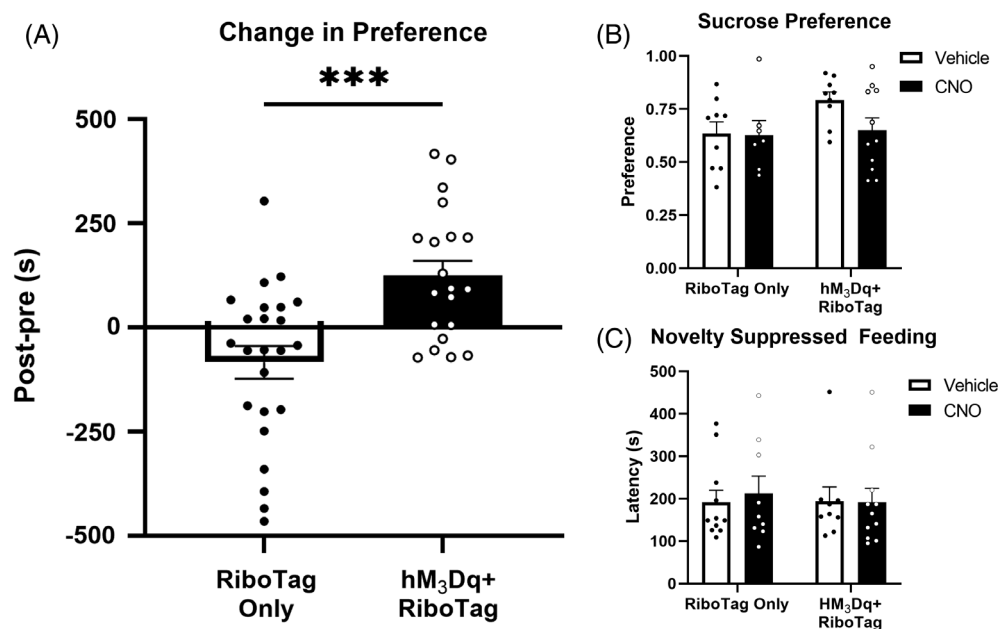
FIGURE 4 Chemogenetic activation of PACAP-expressing neurons in the LHb is directly rewarding. PACAP hM$_3$Dq mice spent significantly more time in the CNO paired side than PACAP RiboTag only mice (A). PACAP hM$_3$Dq mice or PACAP RiboTag only mice did not differ in sucrose preference with or without CNO (B), or latency to eat in the Novelty Suppressed Feeding test (C)

quite distinct effects on fear, anxiety, and approach behaviors. Indeed, future studies are needed to better reconcile these disparities by examining the translatome of these neurons, their inputs, and their electrophysiological responses.

PACAP-expressing neurons are found throughout the brain in both glutamatergic and GABAergic neurons.[54] This recent report examined the colocalization of PACAP expression with glutamate or GABA markers. While PACAP was found in some GABAergic neurons, particularly in the cerebellum, the majority of PACAP-expressing neurons are glutamatergic indicating that these neurons primarily activate downstream targets.[54] Additionally, this report found that nearly all PACAP-expressing neurons and their neighbors also express PAC1, a Gq-coupled receptor and the primary receptor for PACAP, meaning that these neurons may use autocrine and paracrine mechanisms as well as projections to further away targets.[54] Indeed, the Allen Brain Atlas indicates expression of PAC1 in LHb,[55] so activation of PACAP-expressing neurons may lead to local excitation as well.

Responses to stress in the LHb are surprisingly heterogeneous. While roughly one third of neurons in the LHb are activated by footshock, about 10% are actually inhibited.[20] Interestingly, these footshock-inhibited neurons had about twice the resting firing rate as footshock-activated neurons. While the vast majority of LHb neurons are glutamatergic, some express GAD2.[56] Quina and colleagues found these neurons do not appear to package or secrete GABA.[56] Conversely, Flannigan and colleagues showed that optogenetic activation of these GAD2-expressing LHb neurons can induce inhibitory postsynaptic currents in neighboring non-GAD2 cells which are blocked by gabazine, indicating that these cells may be releasing GABA locally.[57] They also have a similar expression and projection pattern to the PACAP-expressing neurons. Furthermore, these GAD2-expressing neurons in the LHb are uniquely active during aggression and on the aggression-paired side of a CPP apparatus, indicating they are involved in the reward learning of aggression.[57]

PACAP has also been shown to disrupt fear memory. ICV administration of PACAP prior to conditioning decreased freezing in rats the next day and notably decreased c-Fos positive neurons in a variety of brain regions including the LHb.[39] Infusion of PACAP$_{6-38}$, a PAC1R antagonist, into the prefrontal cortex of rats decreased freezing to the tone cue, but not the context.[58] This effect was specific to female rats, and the mRNA expression levels of the receptor increased throughout the estrous cycle; however, PACAP mRNA levels did not change with estrous. In humans, a polymorphism of PAC1R increases the risk of PTSD and increases response to fear in the hippocampus and amygdala in women, but not men.[41,59]

Additionally, mice with constitutive knock out of PACAP had no morphine place preference after a single conditioning session, unlike their PACAP positive littermates; however, with two conditioning sessions, they had equal levels of preference.[36] Further, we found that activating these neurons was rewarding, producing a place preference on the CNO-paired side. Additional experiments should investigate whether inhibiting PACAP-expressing neurons in the LHb alters the rewarding properties of opioids.

We tested a small cohort of animals in the open field, where chemogenetic activation of PACAP-expressing neurons in LHb increased locomotion. Previously we used the same hM3Dq DREADD, expressed nonspecifically in rat LHb neurons, where CNO reduced spontaneous (but not motivated) locomotor activity in a dose-dependent fashion.[60] Additionally, a recent report found that chemogenetically activating glutamatergic LHb neurons in mice, or optogenetically activating their terminals to RMTg, but not VTA or DRN, increased susceptibility to isoflurane anesthesia,[61] suggesting that activation of these neurons decreases activity in a variety of models. Thus, the effects of stimulating PACAP-expressing LHb neurons differed from LHb neurons in general. Furthermore, chemogenetic activation of these neurons produced a conditioned place preference but activating these neurons

did not increase the reward associated with sucrose preference or reduce the latency to eat. Thus, it seems that while activating LHb PACAP neurons may be rewarding, activation of these cells does not change the hedonic valence of other rewards or the motivation to consume them. This may be due to a ceiling effect which could be examined in future studies using a lower percentage of sucrose. Additionally, chronically stressing the mice prior to activation of LHb PACAP neurons would be interesting to examine as chronic stress alters sucrose preference and novelty suppressed feeding.[49,62] A caveat to note is that acute antidepressant effects are not observed in novelty suppressed feeding, and chronic treatment of classic antidepressants is needed to affect latency. However, anxiolytics do produce effects immediately in this test.[49] Thus, it may be of interest to activate LHb PACAP neurons chronically prior to testing novelty suppressed feeding.

In summary, LHb PACAP-expressing neurons do not define a distinct phenotypic class of LHb neurons; however, they are unique in behavioral control. These neurons target the RMTg and lateral DRN, as well as the MRN. By targeting these predominantly GABAergic regions, perhaps these neurons are diminishing circuit excitability, which may be responsible for the altered responses in behavior in comparison to whole LHb activation.

ACKNOWLEDGMENTS

DATA AVAILABILITY STATEMENT

The data that support the findings of this study are available from the corresponding author upon reasonable request.

ORCID

Marjorie R. Levinstein https://orcid.org/0000-0003-4360-1503
John F. Neumaier https://orcid.org/0000-0002-1763-7118

REFERENCES

1. Stamatakis AM, Stuber GD. Activation of lateral habenula inputs to the ventral midbrain promotes behavioral avoidance. *Nat Neurosci*. 2012;15(8):1105-1107.
2. Namboodiri VM, Rodriguez-Romaguera J, Stuber GD. The habenula. *Curr Biol*. 2016;26(19):R873-R877.
3. Quina LA, Tempest L, Ng L, et al. Efferent pathways of the mouse lateral habenula. *J Comp Neurol*. 2015;523(1):32-60.
4. Lecca S, Meye FJ, Trusel M, et al. Aversive stimuli drive hypothalamus-to-habenula excitation to promote escape behavior. *Elife*. 2017;6:e30697.
5. Shabel SJ, Proulx CD, Trias A, Murphy RT, Malinow R. Input to the lateral habenula from the basal ganglia is excitatory, aversive, and suppressed by serotonin. *Neuron*. 2012;74(3):475-481.
6. Li B, Piriz J, Mirrione M, et al. Synaptic potentiation onto habenula neurons in the learned helplessness model of depression. *Nature*. 2011;470(7335):535-539.
7. Cerniauskas I, Winterer J, de Jong JW, et al. Chronic stress induces activity, synaptic, and transcriptional remodeling of the lateral

8. Habenula associated with deficits in motivated behaviors. *Neuron*. 2019;104(5):899-915 e898.
8. Proulx CD, Aronson S, Milivojevic D, et al. A neural pathway controlling motivation to exert effort. *Proc Natl Acad Sci USA*. 2018;115(22): 5792-5797.
9. Ootsuka Y, Mohammed M. Activation of the habenula complex evokes autonomic physiological responses similar to those associated with emotional stress. *Physiol Rep*. 2015;3(2):e12297.
10. Gill MJ, Ghee SM, Harper SM, See RE. Inactivation of the lateral habenula reduces anxiogenic behavior and cocaine seeking under conditions of heightened stress. *Pharmacol Biochem Behav*. 2013;111: 24-29.
11. Zhang Q, Feng JJ, Yang S, Liu XF, Li JC, Zhao H. Lateral habenula as a link between thyroid and serotoninergic system modiates depressive symptoms in hypothyroidism rats. *Brain Res Bull*. 2016;124:198-205.
12. Luo XF, Zhang BL, Li JC, Yang YY, Sun YF, Zhao H. Lateral habenula as a link between dopaminergic and serotonergic systems contributes to depressive symptoms in Parkinson's disease. *Brain Res Bull*. 2015; 110:40-46.
13. Nair SG, Strand NS, Neumaier JF. DREADDing the lateral habenula: a review of methodological approaches for studying lateral habenula function. *Brain Res*. 2013;1511:93-101.
14. Coffey KR, Marx RG, Vo EK, Nair SG, Neumaier JF. Chemogenetic inhibition of lateral habenula projections to the dorsal raphe nucleus reduces passive coping and perseverative reward seeking in rats. *Neuropsychopharmacology*. 2020;45(7):1115–1124.
15. Baker PM, Jhou T, Li B, et al. The lateral Habenula circuitry: reward processing and cognitive control. *J Neurosci*. 2016;36(45):11482-11488.
16. Mizumori SJY, Baker PM. The lateral Habenula and adaptive behaviors. *Trends Neurosci*. 2017;40(8):481-493.
17. Thapa R, Donovan CH, Wong SA, Sutherland RJ, Gruber AJ. Lesions of lateral habenula attenuate win-stay but not lose-shift responses in a competitive choice task. *Neurosci Lett*. 2019;692:159-166.
18. Durieux L, Mathis V, Herbeaux K, et al. Involvement of the lateral habenula in fear memory. *Brain Struct Funct*. 2020;225(7):2029-2044.
19. Berger AL, Henricks AM, Lugo JM, et al. The lateral Habenula directs coping styles under conditions of stress via recruitment of the Endocannabinoid system. *Biol Psychiatry*. 2018;84(8):611-623.
20. Congiu M, Trusel M, Pistis M, Mameli M, Lecca S. Opposite responses to aversive stimuli in lateral habenula neurons. *Eur J Neurosci*. 2019; 50(6):2921-2930.
21. Seo JS, Zhong P, Liu A, Yan Z, Greengard P. Elevation of p11 in lateral habenula mediates depression-like behavior. *Mol Psychiatry*. 2018; 23(5):1113-1119.
22. Hu H, Cui Y, Yang Y. Circuits and functions of the lateral habenula in health and in disease. *Nat Rev Neurosci*. 2020;21(5):277-295.
23. Matsumoto M, Hikosaka O. Representation of negative motivational value in the primate lateral habenula. *Nat Neurosci*. 2009;12(1):77-84.
24. Wirtshafter D, Asin KE, Pitzer MR. Dopamine agonists and stress produce different patterns of Fos-like immunoreactivity in the lateral habenula. *Brain Res*. 1994;633(1–2):21-26.
25. Brinschwitz K, Dittgen A, Madai VI, Lommel R, Geisler S, Veh RW. Glutamatergic axons from the lateral habenula mainly terminate on GABAergic neurons of the ventral midbrain. *Neuroscience*. 2010; 168(2):463-476.
26. Geisler S, Trimble M. The lateral habenula: no longer neglected. *CNS Spectr*. 2008;13(6):484-489.
27. Bernard R, Veh RW. Individual neurons in the rat lateral habenular complex project mostly to the dopaminergic ventral tegmental area or to the serotonergic raphe nuclei. *J Comp Neurol*. 2012;520(11): 2545-2558.
28. Goncalves L, Sego C, Metzger M. Differential projections from the lateral habenula to the rostromedial tegmental nucleus and ventral tegmental area in the rat. *J Comp Neurol*. 2012;520(6):1278-1300.

29. Kalen P, Strecker RE, Rosengren E, Bjorklund A. Regulation of striatal serotonin release by the lateral habenula-dorsal raphe pathway in the rat as demonstrated by in vivo microdialysis: role of excitatory amino acids and GABA. *Brain Res*. 1989;492(1–2):187-202.

30. Levinstein MR, Coffey KR, Marx RG, Lesiak AJ, Neumaier JF. Stress induces divergent gene expression among lateral habenula efferent pathways. *Neurobiol Stress*. 2020;13:100268.

31. Christensen T, Jensen L, Bouzinova EV, Wiborg O. Molecular profiling of the lateral habenula in a rat model of depression. *PLoS One*. 2013; 8(12):e80666.

32. Hashikawa Y, Hashikawa K, Rossi MA, et al. Transcriptional and spatial resolution of cell types in the mammalian Habenula. *Neuron*. 2020;106:1-16.

33. Wagner F, French L, Veh RW. Transcriptomic-anatomic analysis of the mouse habenula uncovers a high molecular heterogeneity among neurons in the lateral complex, while gene expression in the medial complex largely obeys subnuclear boundaries. *Brain Struct Funct*. 2016;221(1):39-58.

34. Hannibal J. Pituitary adenylate cyclase-activating peptide in the rat central nervous system: an immunohistochemical and in situ hybridization study. *J Comp Neurol*. 2002;453(4):389-417.

35. Hashimoto H, Shintani N, Tanida M, Hayata A, Hashimoto R, Baba A. PACAP is implicated in the stress axes. *Curr Pharm des*. 2011;17(10): 985-989.

36. Marquez P, Bebawy D, Lelievre V, et al. The role of endogenous PACAP in motor stimulation and conditioned place preference induced by morphine in mice. *Psychopharmacology (Berl)*. 2009;204(3): 457-463.

37. Stroth N, Holighaus Y, Ait-Ali D, Eiden LE. PACAP: a master regulator of neuroendocrine stress circuits and the cellular stress response. *Ann N Y Acad Sci*. 2011;1220:49-59.

38. Hammack SE, Cheung J, Rhodes KM, et al. Chronic stress increases pituitary adenylate cyclase-activating peptide (PACAP) and brain-derived neurotrophic factor (BDNF) mRNA expression in the bed nucleus of the stria terminalis (BNST): roles for PACAP in anxiety-like behavior. *Psychoneuroendocrinology*. 2009;34(6):833-843.

39. Meloni EG, Venkataraman A, Donahue RJ, Carlezon WA Jr. Bi-directional effects of pituitary adenylate cyclase-activating polypeptide (PACAP) on fear-related behavior and c-Fos expression after fear conditioning in rats. *Psychoneuroendocrinology*. 2016;64:12-21.

40. Telegdy G, Adamik A. Neurotransmitter-mediated anxiogenic action of PACAP-38 in rats. *Behav Brain Res*. 2015;281:333-338.

41. Ressler KJ, Mercer KB, Bradley B, et al. Post-traumatic stress disorder is associated with PACAP and the PAC1 receptor. *Nature*. 2011; 470(7335):492-497.

42. Jovanovic T, Stenson AF, Thompson N, et al. Impact of ADCYAP1R1 genotype on longitudinal fear conditioning in children: interaction with trauma and sex. *Neuropsychopharmacology*. 2020;45(10):1603-1608.

43. Harris JA, Hirokawa KE, Sorensen SA, et al. Anatomical characterization of Cre driver mice for neural circuit mapping and manipulation. *Front Neural Circuits*. 2014;8:76.

44. Coffey KR, Barker DJ, Ma S, West MO. Building an open-source robotic stereotaxic instrument. *J Vis Exp*. 2013;80:e51006.

45. Lesiak AJ, Brodsky M, Neumaier JF. RiboTag is a flexible tool for measuring the translational state of targeted cells in heterogeneous cell cultures. *Biotechniques*. 2015;58(6):308-317.

46. Lesiak AJ, Neumaier JF. RiboTag: not lost in translation. *Neuropsychopharmacology*. 2016;41(1):374-376.

47. Lesiak AJ, Coffey K, Cohen J, Liang KJ, Chavkin C, Neumaier JF. Sequencing the serotonergic neuron translatome reveals a new role for Fkbp5 in stress. *Mol Psychiatry*. 2021;26(9):4742–4753.

48. Samuels BA, Anacker C, Hu A, et al. 5-HT1A receptors on mature dentate gyrus granule cells are critical for the antidepressant response. *Nat Neurosci*. 2015;18(11):1606–1616.

49. Samuels BA, Hen R. Novelty-suppressed feeding in the mouse. In: Gould TD, ed. *Mood and anxiety related phenotypes in mice: Characterization using behavioral tests*. Vol 2. Humana Press; 2011:107-121.

50. Jo YS, Heymann G, Zweifel LS. Dopamine neurons reflect the uncertainty in fear generalization. *Neuron*. 2018;100(4):916-925 e913.

51. Abraham AD, Schattauer SS, Reichard KL, et al. Estrogen regulation of GRK2 inactivates kappa opioid receptor signaling mediating analgesia, but not aversion. *J Neurosci*. 2018;38(37):8031-8043.

52. Ferguson SM, Phillips PE, Roth BL, Wess J, Neumaier JF. Direct-pathway striatal neurons regulate the retention of decision-making strategies. *J Neurosci*. 2013;33(28):11668-11676.

53. Armbruster BN, Li X, Pausch MH, Herlitze S, Roth BL. Evolving the lock to fit the key to create a family of G protein-coupled receptors potently activated by an inert ligand. *Proc Natl Acad Sci USA*. 2007; 104(12):5163-5168.

54. Zhang L, Hernandez VS, Gerfen CR, et al. Behavioral role of PACAP signaling reflects its selective distribution in glutamatergic and GABAergic neuronal subpopulations. *Elife*. 2021;10:e61718.

55. Lein ES, Hawrylycz MJ, Ao N, et al. Genome-wide atlas of gene expression in the adult mouse brain. *Nature*. 2007;445(7124): 168-176.

56. Quina LA, Walker A, Morton G, Han V, Turner EE. GAD2 expression defines a class of excitatory lateral Habenula neurons in mice that project to the raphe and Pontine Tegmentum. *eNeuro*. 2020;7(3): ENEURO.0527–19.2020.

57. Flanigan ME, Aleyasin H, Li L, et al. Orexin signaling in GABAergic lateral habenula neurons modulates aggressive behavior in male mice. *Nat Neurosci*. 2020;23(5):638-650.

58. Kirry AJ, Herbst MR, Poirier SE, et al. Pituitary adenylate cyclase-activating polypeptide (PACAP) signaling in the prefrontal cortex modulates cued fear learning, but not spatial working memory, in female rats. *Neuropharmacology*. 2018;133:145-154.

59. Stevens JS, Almli LM, Fani N, et al. PACAP receptor gene polymorphism impacts fear responses in the amygdala and hippocampus. *Proc Natl Acad Sci U S A*. 2014;111(8):3158-3163.

60. Nair SG, Smirnov DS, Estabrook MM, Chisholm AD, Silva PR, Neumaier JF. Effect of chemogenetic inhibition of lateral habenula neuronal activity on cocaine- and food-seeking behaviors in the rat. *Addict Biol*. 2021;26(1):e12865.

61. Liu C, Liu J, Zhou L, et al. Lateral Habenula Glutamatergic neurons modulate Isoflurane anesthesia in mice. *Front Mol Neurosci*. 2021;14: 628996.

62. Liu MY, Yin CY, Zhu LJ, et al. Sucrose preference test for measurement of stress-induced anhedonia in mice. *Nat Protoc*. 2018;13(7): 1686-1698.

SUPPORTING INFORMATION

Additional supporting information may be found in the online version of the article at the publisher's website.